THE UNIVERSITY OF
NEW SOUTH WALES

**SCHOOL OF ELECTRICAL ENGINEERING
AND TELECOMMUNICATION**

Resource Allocation and Practical Energy Harvesting Model for Wireless Power Communication Systems

Author: Zhechao Cai

Thesis submitted as a requirement for the degree
Bachelor of Engineering (Electrical Engineering)

Submitted: 12th July 2017

Abstract

With the vast development of energy harvesting technologies, wireless energy transmission techniques have been widely developed. One of the most potential solution to provide sustained network operation to ambient sensor nodes is the devoted radio frequency (RF) power source. The transmitter can be deployed more flexibly and the its working lifetime can be extended using this source. In this thesis, we would study the characterization of RF power source in charging procedure to determine the behavior of RF energy transfer(RFET) with a distinctive charging scheme comparing to the normal steady voltage charging since its providing steady power from the supply source to the storage element. Moreover, the relationship between charging time, input power and output power is proposed and simulated. By using this model the output RF power can be computed by given certain input RF power and certain charging time. In terms of resource allocation, we compare two energy allocation schemes(Zero-Forcing(ZF) and Maximum ratio transmission(MRT)) to analyze the difference regards to achievable sum rate(ASR) and required downlink transmit power(DTP) under the same condition and assumptions. The simulated results imply that ZF is performing better than MRT under the same condition, which is coinciding with the theoretical result.

Acknowledgements

First of all, I would take this opportunity to express my greatest gratitude to my supervisor, Dr. Derrick Wing Kwan Ng for all his help, advice, support, and encouragement. This dissertation would have been impossible without his guidance. Derrick has not only advised me on how to pursue great research, but also helped me to explore my strengths to succeed and even finding the ultimate goal of my life. His help goes far beyond this dissertation.

Also, I would like to thank Ken Xiaodong Zhang and Allen Yicong Cao for all the valuable suggestions and discussions that really improved this dissertation. They helped me a lot in finalizing this project within the limited time frame and assisted me on using latex studio to write this formal thesis. I would like to thank my families for encouraging me to study in Australia and supporting me throughout my university study. Their love and prayers gave me strength to overcome difficulties throughout this endeavor.

Contents

Abbreviations

AGWN	**A**dditive **G**aussian **W**hite **N**oise
ASR	**A**chievable **S**um **R**ate
CSI	**C**hannel **S**tate **I**nformation
DTP	**D**ownlink **T**ransmit **P**ower
IDEM	**I**ntegrated **D**ata and **E**nergy **M**ule
MIMO	**M**ultiple-**I**nput **M**ultiple-**O**utput
MRT	**M**axium **R**atio **T**ransmission
RF	**R**adio **F**requency
RFET	**R**adio **F**requency **E**nergy **T**ransfer
SINR	**S**ignal-to-**I**nterference-plus-**N**oise **R**atio
WSN	**W**ireless **S**ensor **N**etworks
ZF	**Z**ero-**F**orcing

List of Figures

Chapter 1

Introduction

1.1 Energy Harvesting

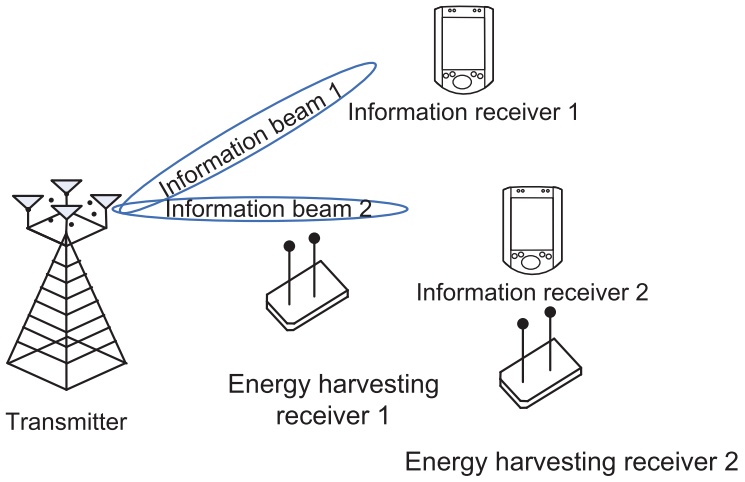

FIGURE 1.1: Simple Wireless Energy Transfer Example [1]

In remote sensor networks, communication of the sensor and the base station, detecting, sensing and storage would consume energy. If the energy inside the battery in the sensor run out, the deployed sensor would be quite difficult to be accessed and to be replaced the batteries. Therefore, there are some recent works have concentrated on developing persistent operating sensor nodes by wirelessly powering it in order to provide minimized power. There are some natural resources like solar power [5][6][7], wind power [8], vibration power [9], ambient radio frequency source [10]–[28] and getting power from human activities [29] which would provide energy to ambient sensors wirelessly have been chosen and tested. However, these kinds of resources cannot guarantee on providing sufficient energy to ambient environment

under all conditions. Therefore, these sources are currently not relatively reliable for prolonged sensor network system [30].

One of significant potential solution the deal with this ambient resource uncertainty is the dedicated RFET [31]. Be that as it may, the accomplishment of RFET depends on precisely anticipating the charging effectiveness and power level during limited time used for charging. This is especially critical in integrated data and energy mule (IDEM) exemplification [32], which develops the idea of the ordinary data mule [33]. By advancing the previous data mule, this new exemplification becomes especially critical in integrated data and energy mule(IDEM). The adjacent or surrounded field nodes would be visited frequently by this innovative paradigm, i.e. IDEM and a node would be also placed by it for collecting information remotely and recharging it via energy transferred in RF. Since the remaining power strength at a node is undefined and irregular, characterizing the charging time and power would be useful for maximize the efficacy and help us to customize the charging property.

Its critical for the charging operation if we can estimate the energy level of the field sensor. To propel this issue, we consider the charging is doing on a basic R-C circuit and the energy conserving unit is just a simple supercapacitor [3]. We would have to characterize the charging time property of the circuit to find out the efficiency of this dedicated radio frequency energy transfer(RFET).

Unlike regular powering of a normal capacitor from a steady voltage supply source like dc supply, the RFET model is using constant power source. When the capacitor is charged by a consistent voltage source, the beginning current is large, and then slowly decrease to small value then to zero because of energizing charged capacitor by the supply voltage. Using V_0 to denote the supply voltage source, the expression for the current and voltage across an supercapacitor in a normal series Resistor-Capacitor circuit is shown here [34]

$$V_C(t) = V_0[1 - e^{\frac{-t}{RC}}] \qquad I(t) = \frac{V_0}{R} e^{\frac{-t}{RC}} \tag{1.1}$$

There are a few distinctions between the conventional charging and RF charging. The most fundamental one is that the in conventional charging circuit, the supply voltage is fixed at a certain value and it would not change till the completion of charging. However, the second one is using constant power to charge the super-capacitor. As increasing the supply voltage in the circuit, the current across the

capacitor would decrease because the constant input power. Since the power across the load is also constant, the voltage across it would increase. Therefore, it come out with that if we increase the supply voltage (keeping input power constant), the voltage across the load would increase accordingly. To this end, we proposed expressions for characterizing the relationship between input power, charging time and output power.

1.2 Resource Allocation

With the advancement in wireless powered communication MIMO system, the demand of wireless data transmission service has increased enormously. Due to the cost on the radio spectrum, the bandwidth is usually constrained. By increasing the transmission data rate, in a way the power consumption on the receivers can be reduced without enlarging the bandwidth, the wireless sensors network(WSN) can be more efficient and the bandwidth can be easier to be controlled [35]. To achieve this demand, its can be widely seen that multiple-input multiple-output(MIMO) system has been implemented and developed because of its capacity to cause the power consumption less costly and increase the spectral.

One of the most improvement of MIMO technique is the massive MIMO technique with the increasing demand of bandwidth capacity. This technique is basically a multiuser MIMO system with massive amount of base station antennas with lots of antennas serving concurrently in those antennas [36]. To some extent it keeps all the advantages of conventional MIMO technique and improve its behavior in aspects such as energy and bandwidth efficiency, interference reduction and reliability [37]. Moreover, by using great amount of antennas in massive MIMO technique, multiuser processing can be further simplified and thermal noise and fast fading can be vanished [37].

Chapter 2

Literature Review

Motivated by the growing concern on power consumption in wireless communication systems, green communication is a new concept proposed in recent years, which aims to reduce the consumption of the traditional fossil energy. To convert green communications from concept to reality, green communication techniques have been intensively investigated in the past years, including the research perspectives on energy efficient devices (e.g., energy-efficient RF module), employment of renewable energy sources, energy-minimizing adaptive transmission, interference management and mitigation, energy-efficient routing and multihop, and so on [38][39][40][41, 42]–[43], as illustrated in Fig 2.1. Specifically, the green communication techniques have the common objective of improving the energy-efficiency.

In addition to the use of energy-efficient devices, energy-efficient adaptive transmission is an effective technique to improve the energy efficiency for a single transmitter [44]–[56]. By adapting the transmitters parameters (e.g., the constellation signaling, the number of diversity branches, etc.) to the channel condition, the adaptive transmission can trade off between the energy efficiency and spectral efficiency under the performance constraints [57]. For a network with multiple transmitters, the interference management and mitigation technique can be used to mitigate the interference level at the receivers so that the transmission energy at the transmitters can be reduced accordingly without compromising the SINR of the wireless link [38]. Moreover, on network level, using the energy-efficient routing and multihop techniques, information exchanges between two transceivers (e.g., the base station and mobile terminal) can be realized by multiple relays with better channel conditions. Since the information is transmitted over better channels, the same rate can be achieved with lower transmission energy [38].

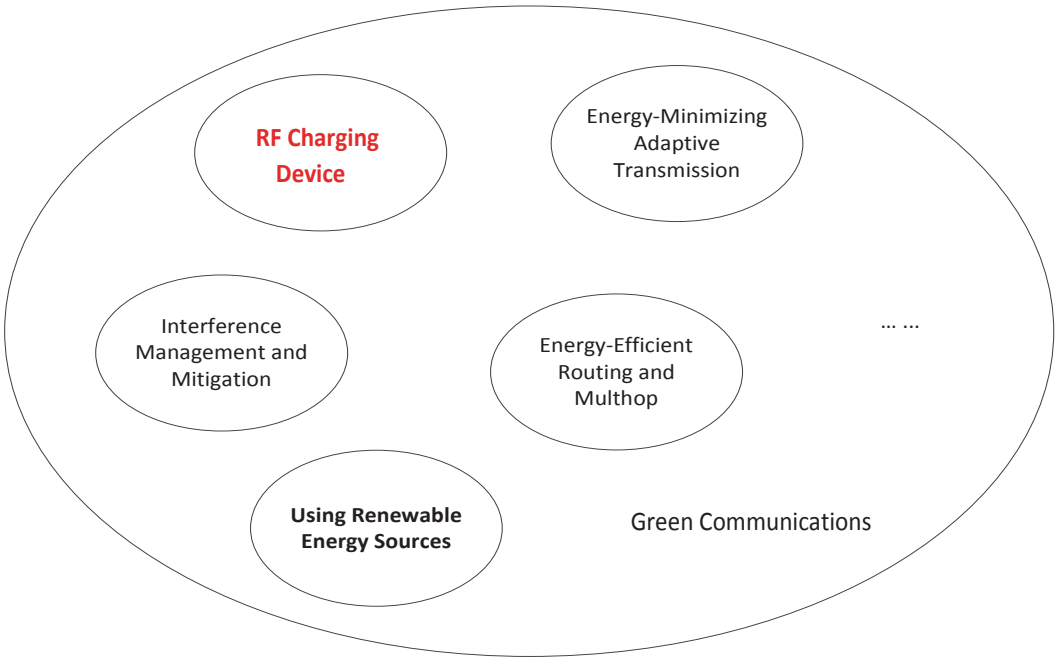

FIGURE 2.1: Research perspectives on green wireless communications

Employing the renewable energy is a novel way to realize green communications, which is motivated by the rapid development of the energy harvesting techniques in recent years. For energy harvesting communications, the employment of the energy harvesting transmitters can not only avoid the use of the traditional fossil energy but also provide the exible deployment and perpetual operation [58] [59]. Due to the limited capability of the energy harvesting and storage, energy harvesting communications require the best use of the harvested energy, balancing the communication performance and the potential energy outage and overow caused by the energy harvesting dynamics [60], which is different from some traditional techniques that realize the improvement on energy efficiency by solely reducing the energy consumption.

Energy harvesting transmitter is the fundamental unit of the energy harvesting communication system, typically consisting of the energy harvesting module, energy storage module, and transmitter module [60][58] , as shown in Fig 2.2. The energy harvesting module harvests ambient energy from the surrounding environment and stores it in the energy storage module, which could be a rechargeable battery or supercapacitor. The storage module powers the transmitter, which contains the processor, sensing and radio blocks. Specifically, the sensing block performs the sensing functionality, e.g., collecting the environment information, depending on the application, and the radio block transmits the information processed by the

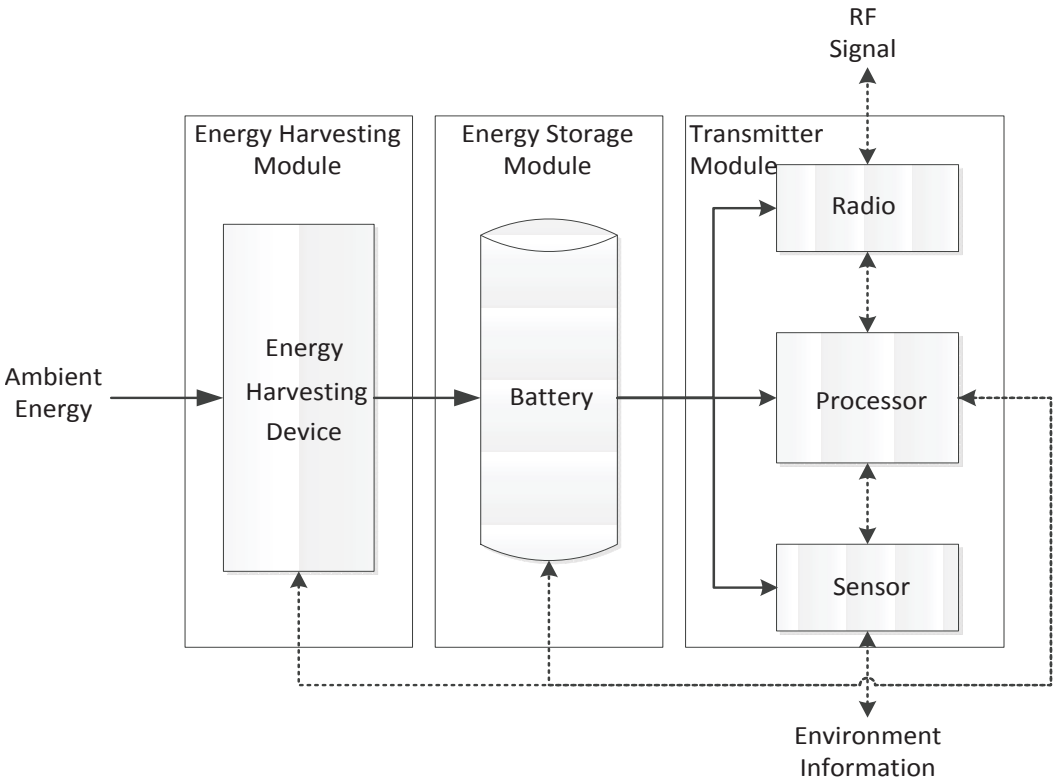

FIGURE 2.2: The high-level block diagram of a typical energy harvesting transmitter

processor and receives the data from the control center or another transmitters. In particular, in addition to processing the information, the processor is also the control unit of the energy harvesting transmitter, controlling the transmitters working status, e.g., the transmitting or receiving status, the modulation and code scheme, and the transmission power.

Using the renewable energy is the most important feature of the energy harvesting transmitter and we can characterize the transmitters operation (e.g., use specific transmission policy) in terms of the energy consumption by the energy expenditure curve (i.e., the integration of the energy expenditure over time) along with its feasible region [61], as shown in Fig 2.3. Specifically, each energy expenditure curve corresponds to a particular communication performance and must be in the feasible region constrained by the energy harvesting process and the battery capacity. It is easy to understand that the feasible region is upper-bounded by the accumulative energy harvesting curve (i.e., the integration of the harvested energy over time) such that the accumulated energy expenditure cannot exceed the accumulated energy harvesting for all time otherwise the battery level would be negative. Also, the

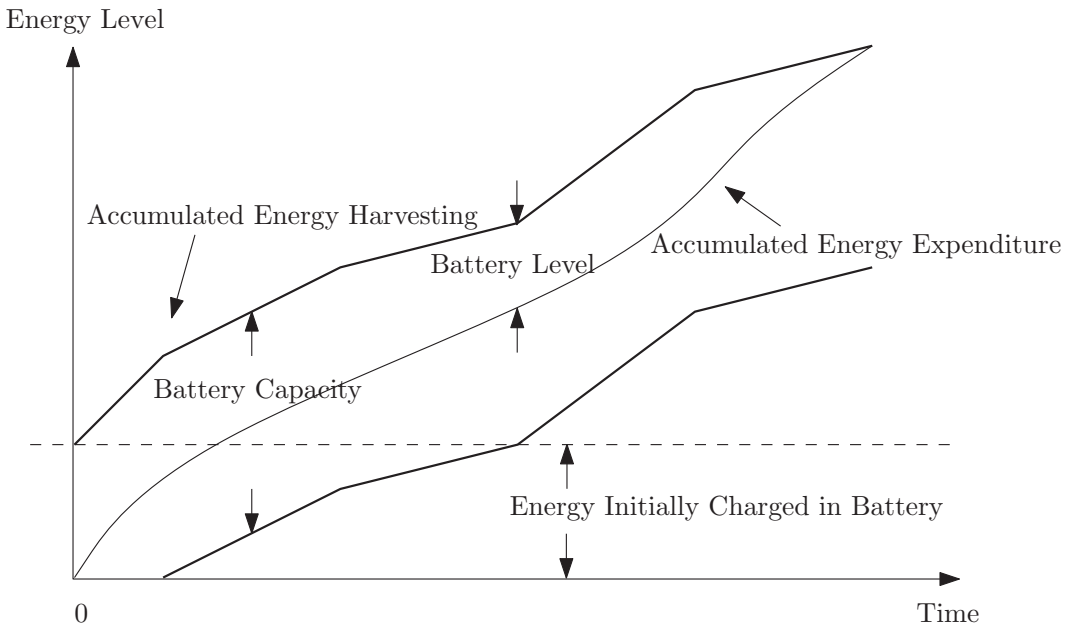

FIGURE 2.3: The energy expenditure curve and its feasible region.

energy expenditure curve cannot be below the curve formed by subtracting the battery capacity from the accumulated energy harvesting (or zero, whichever is larger) since the battery level cannot exceed its capacity [61].

For traditional grid- and battery-powered transmitters, we can also use the similar way to characterize their energy expenditure curves along with the feasible regions; however, we will see that their curves and feasible regions are quite different from those of the energy harvesting transmitter. Specially, for the grid-powered transmitter subject to the maximum transmission power, its energy expenditure curve is continuous and the derivative (both left- and right-derivatives at the non-differentiable point) cannot exceed the value of the maximum transmission power; for the battery-powered transmitter, since the energy is not replenishable, its energy expenditure curve must stay below a constant horizon line (e.g., the dashed line in Fig 2.3) that represents the energy initially charged in the battery. Note that, since the different energy expenditure curves represent different operation schemes and correspond to the different communication performances, the energy harvesting transmitters operate significantly differently as compared to the grid- and battery-powered transmitters. Therefore, lots of interesting and changeling research issues arise for the energy harvesting transmitters, including the architecture design of energy harvesting transmitter, channel capacity of energy harvesting communications, resource allocation, routing and relay selection for energy harvesting networks, and so on, as illustrated in Fig 2.4.

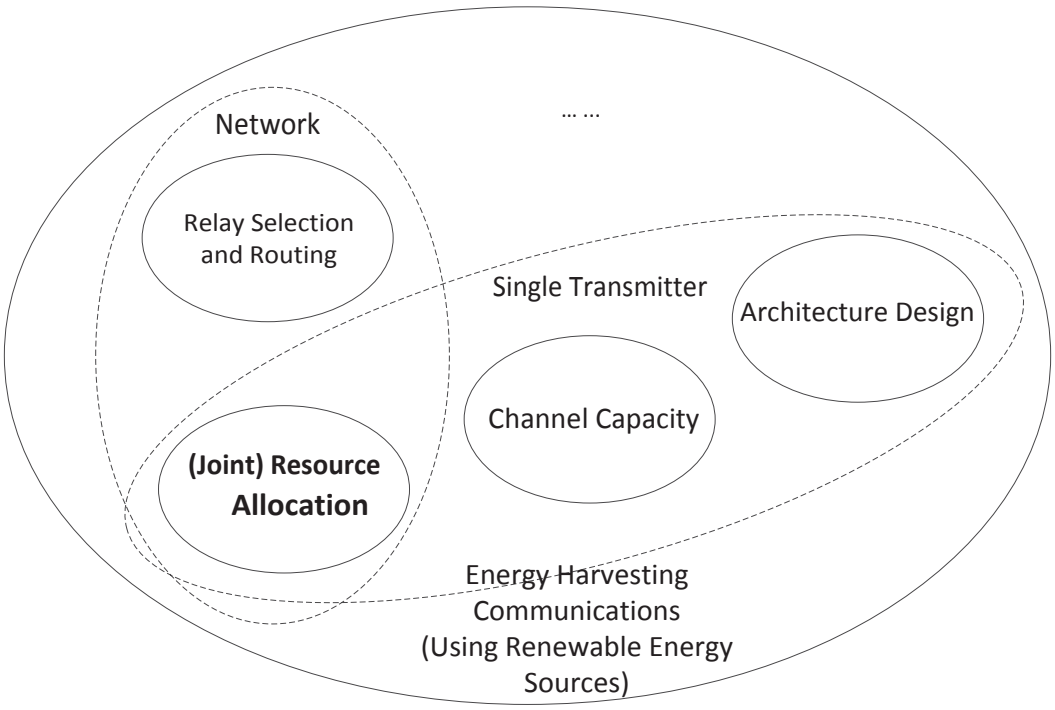

FIGURE 2.4: Research perspectives on energy harvesting communications.

For energy harvesting transmitters, the architecture design is the most essential issue, i.e., how to design the energy harvesting transmitter based on the specific application. Since the energy harvesting transmitter is ideally expected to work perpetually, we need to design and adapt the energy harvesting, modulation, and sensing techniques to strike a balance between the communication performance required by the specific application and the system reliability affected by the potential energy outage. The architecture design was addressed by lots of works [62][58]. Specifically, the energy-harvesting active networked tags (EnHANTs) were developed in [63] and [64]as small devices that can be attached to small objects that are not traditionally networked.

Channel capacity is an interesting and challenging theoretical topic for energy harvesting communications, which provides the theoretical bounds on the performance. Unlike the traditional battery-powered systems, energy arrival of the energy harvesting transmitter is a random process over the symbol durations and the harvested energy is not necessarily consumed up immediately. On the other hand, when the battery is empty, the transmission has to be interrupted. Thus energy harvesting communications require a major shift in terms of the energy constraint imposed on the channel input compared to those in the existing literature. Specically, the

channel capacities for energy harvesting communications were discussed in [65] with various energy conditions for various channels.

At the transmitter-end, the resource allocation is key to make the best use of the harvested energy, ensuring the quality, long-term, and uninterrupted communications. With the battery, the harvested energy can be used immediately or stored for future transmission. Therefore, by properly choosing the energy allocation policy, the transmitter may use the energy to receive its maximum marginal utility, e.g., sum-rate. Moreover, in energy harvesting networks, joint resource allocation, e.g., the joint energy and spectral resource allocation, can provide additional degrees of freedom for optimization, thus the harvested energy may be better utilized for achieving an outperformed performance. The resource allocation for energy harvesting communications is widely investigated in the past years, which is also the subject of this thesis. We will provide a detailed literature review for the existing resource allocation techniques in the next section.

On network level, the studies of the relay selection and routing are also interesting for energy harvesting communications, which aim to effectively schedule the data transmissions in the energy harvesting networks. Specifically, in energy harvesting networks, the energy consumed by the transmitter is mostly harvested from the surrounding environment rather than the energy initially charged in the battery. Thus, the traditional relaying and routing policies have to be revised in order to decide how to deliver packets using the harvested energy efficiently for perpetual operation. This requires a paradigm shift in the design of relaying and routing algorithms. For example, [66] investigate the relaying and routing policies for energy harvesting communications.

Moreover, some new research topics emerged for energy harvesting communications recently. For example, incorporating the energy harvesting transmitter with the cellular network, [67] discussed the availability of the energy harvesting base station in multi-tier heterogeneous cellular networks. The topology planning problem was considered in [68] for the cellular networks enhanced by energy harvesting. Instead of passively harvesting the ambient energy, an interesting and challenging scenario arises when the transmitter performs simultaneous wireless information and power transfer [69]. It leads to the open problem for joint power control and user scheduling, energy and information scheduling, and interference management [59].

In this paper, we will focus on energy harvesting in RF charging area. From [7] - [30], [70]–[80], we can conclude that the sensor nodes cannot stay awake for a

prolonged time since the charging rate of ambient source is normally much lower than the sensor energy consumption rate. It would need to shut down for a while to recharge then return to its normal operation. In addition, since the charging environment is not always compatible for wireless charging, we would need to find out a better wireless charging technique. Here is the comparison diagram provided in [30].

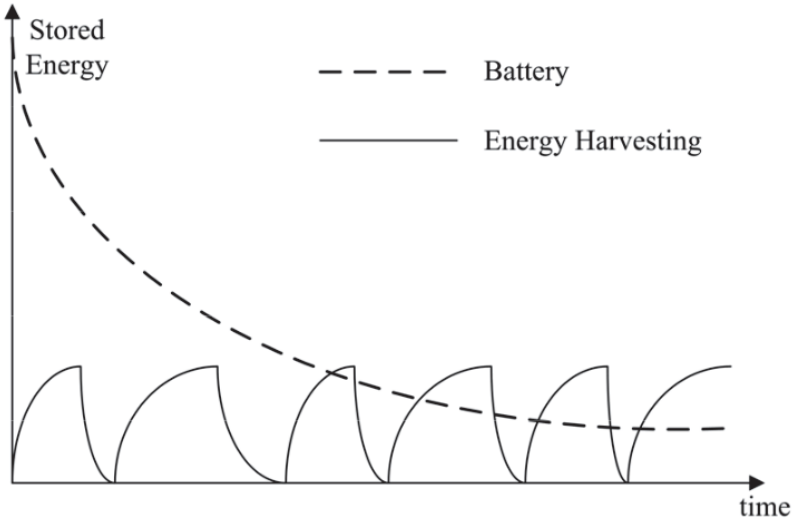

FIGURE 2.5: Battery Charging Versus Normal Ambient Source Charging[2]

As we can see from Fig 2.5, in spite of some disadvantages of charging from a battery, it's still more efficient and steady than regular charging from ambient source. Therefore, building up a dedicated RFET model is a nontrivial task for developing a reliable ambient charging source.

In [81], to reduce the RF charging delay in the network, an ideal movement technique of the wireless charger was proposed. In [82], a rechargeable wireless sensor network with common energy-minimizing routing and energy-balanced radio frequency charging scheme was proposed. Nevertheless, each of them is under steady charging rate and relied on a linear charging model which is simplified and empirical.

To our best knowledge and undergoing sufficient research on past papers, it can be summarized that currently there is no existing model available in the area of RF charging time characterization. Our final RF charging model briefly is aiming to fill up this knowledge gap and offering a reliable system for breaking down the efficacy of the RFET network with portable charging units to provide prolonged system operation[32].

In [83], a systematic solution for steady energy loading of supercapacitors is mentioned. Its slightly different from our model since its about constant power de-energizing rather than constant power energizing. Furthermore, [84] proposed an analytical equation for supply voltage for steady power charging. However, it did not purpose the equation expressing the relationship between the voltage expression of the capacitor and charging time. This is required for describing the charging time characterization. There are uncountable past works focusing on constant voltage charging whereas not much analytical formulations on steady power charging can be found.

Chapter 3

System Model

3.1 Energy Harvesting Model

The energy harvesting procedure is divided into two steps, firstly the energy is transmitted from the base station to the receivers, the receiver is considered as RF powered sensors. Secondly, the harvested power by the sensor is deployed to a P1110 functional block which can be regarded as a normal R-C circuit. In this stage the received RF power is used to charged the supercapacitor in the circuit. Our ultimate goal is to find out the variation of the voltage across the supercapacitor.

3.1.1 Energy Harvesting Stage One

According to [1], the received RF power by the sensor in the wireless powered system is not linear to the input RF power and the relationship between them can be expressed by Equations 3.1 and 3.2. Although the conventional logistic Equation 3.2 with respect to the sensor RF power P_{ER_j} can also illustrate the logistic relationship however it does not start from the origin. Since with zero input RF power, the output RF power needs to be absolute zero, we introduce this parameter Ω_j in Equation 3.1 to achieve this need. In these expressions, the maximum received power at ER_j is denoted by constant M_j and a_j and b_j are parameters denoting specific circuit characteristics like capacitances, resistance and inductance. Generally speaking, the EH hardware circuit of each energy receivers is fixed so M_j, a_j and b_j can be simply found by using a normal curve fitting functional tool.

$$\Phi_{ER_j}^{Practical} = \frac{\Psi_{ER_j}^{Practical} - M_j\Omega_j}{1-\Omega_j}, \quad \Omega_j = \frac{1}{1+exp(a_j b_j)} \tag{3.1}$$

$$\Psi_{ER_j}^{Practical} = \frac{M_j}{1+exp(-a_j(P_{ER_j} - b_j))} \tag{3.2}$$

3.1.2 Energy Harvesting Stage Two

In stage two, In order to build up the three-dimension model and find out the relationship between charging time, input power and output power, we would need to build up a system model to simulate the process of employing the receiver RF energy received(i.e. Φ_{ER_j} in Equation 3.1) from stage one and utilize it in a proposed functional block.

As a unique example of steady power charging using RFET, the power obtained for charging the ultracapacitor is kept unchanged for an RF source(with fixed transferring RF power) from fixed interval. According to [85][3], we can consider the charging energy is delivered to a operation box and here we consider it as the P1110 functional block. It is operating at 915.0 MHz and harvesting RF source power from -5 to 20 dBm. This functional block would transfer RF energy received from stage one to dc power and it can be used to power a circuit or just stored in a supercapacitor. As we mentioned before, in constant power charging paradigm increasing the input voltage would increase the voltage across the load accordingly. As we can see in Fig 3.1, the voltage across the load is V_{OUT}, which is equal to to the supply voltage in Fig 3.2. Therefore, charging this P1110 functional block is equivalently charging the equivalent normal R-C circuit as shown in Fig 3.2. The capacitor here can be regarded as a normal sensor which is fetching energy from the base station. As long as we can find out the relationship between the input RF power from the base station, the charging time and the output RF power delivered to the supercapacitor, we can be acquainted with the characteristic of the charging procedure and by utilizing these features we can actually control the behavior of the sensors. As a result, it could significantly simplify and optimize the design procedure of RF charging via wireless communication network hence power consumptions can be reduced to relatively low level.

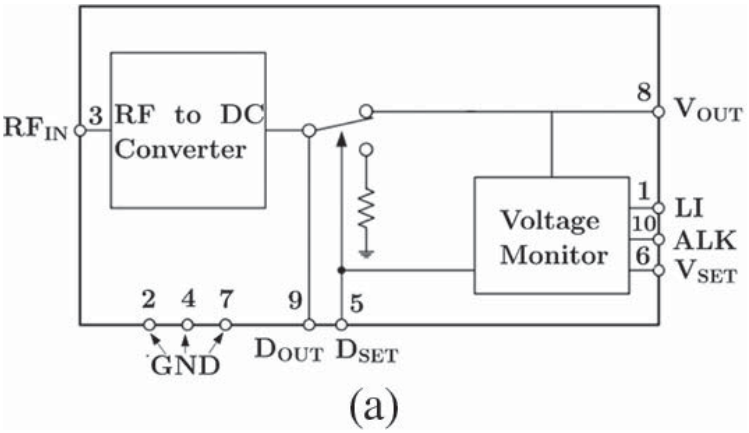

FIGURE 3.1: P1110 Functional Block[3]

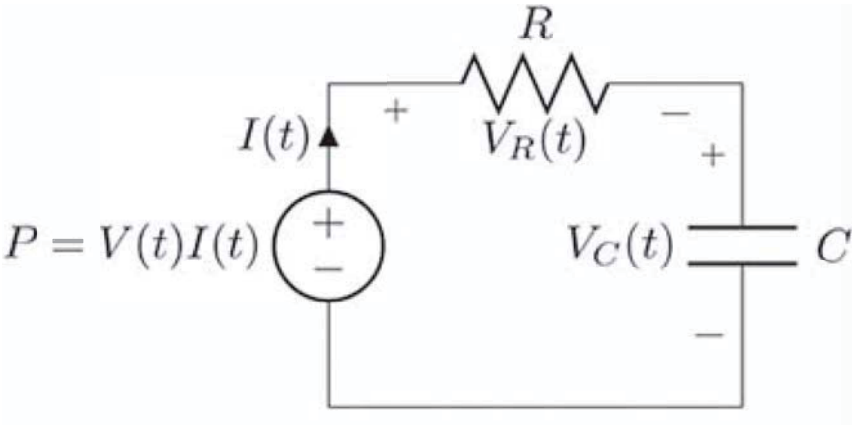

FIGURE 3.2: The Equivalent Normal R-C Circuit[3]

Using Kirchhoff's voltage law in the equivalent normal R-C circuit in Fig 3.2 we get the Equations shown in 3.3:

$$\begin{aligned} V(t) &= V_R(t) + V_C(t) \\ P &= V(t) \cdot I(t) = [V_R(t) + V_C(t)] \cdot I(t) \\ &= R \cdot (\frac{dQ}{dt})^2 + \frac{Q}{C} \cdot \frac{dQ}{dt} \end{aligned} \tag{3.3}$$

To further simplify this equation, we the simplification provided in [3], we can ultimately achieve the expression for representing the voltage and current across the supercapacitor as we can see in Equation 3.4 and 3.5[3]

$$V_C(t) = \frac{2\sqrt{RP}(1 - \frac{1}{Z})}{\sqrt{1 - (1 - \frac{1}{Z})^2}} \tag{3.4}$$

$$I(t) = \frac{dQ}{dt} = \frac{-\frac{Q(t)}{C} + \sqrt{(\frac{Q(t)}{C})^2 + 4RP}}{2R} \tag{3.5}$$

Where

$$Z = \frac{1}{2}[1 + W_0(e^{1+\frac{2t}{RC}})] \tag{3.6}$$

and

$$Q(t) = \frac{2C\sqrt{RP}(1 - \frac{1}{Z})}{\sqrt{1 - (1 - \frac{1}{Z})^2}} \tag{3.7}$$

As we can see in Equation 3.4, the output voltage across the capacitor is with respect to the input RF transmitting power and parameter Z, which depends on the charging time as shown in Equation 3.6. Moreover, the current as shown in Equation 3.5 is with respect to the input RF power and the parameter Q shown in Equation 3.7 is related to Z again. This implies that both of the voltage and current are related to these two variables, input RF transmitting power and charging time. In order to find out the output power across the capacitor, we just need to simply multiply the output voltage by the current across it. Because the multiplication is done in the matrix form, we are using dot product as shown in Equation 3.8. Apparently the output received RF power P_{OUT} across the supercapacitor is a variable depends on t and P_{IN}. By finding the relationship between those three parameters, we can ultimately control the behavior of this energy harvesting process and to some extent a more efficient and less costly energy harvesting model can be developed upon using the characteristics and the behavior of this model.

$$P_{OUT}(t, P_{IN}) = V_C(t) \cdot I(t) \tag{3.8}$$

3.2 Resource Allocation Channel Model

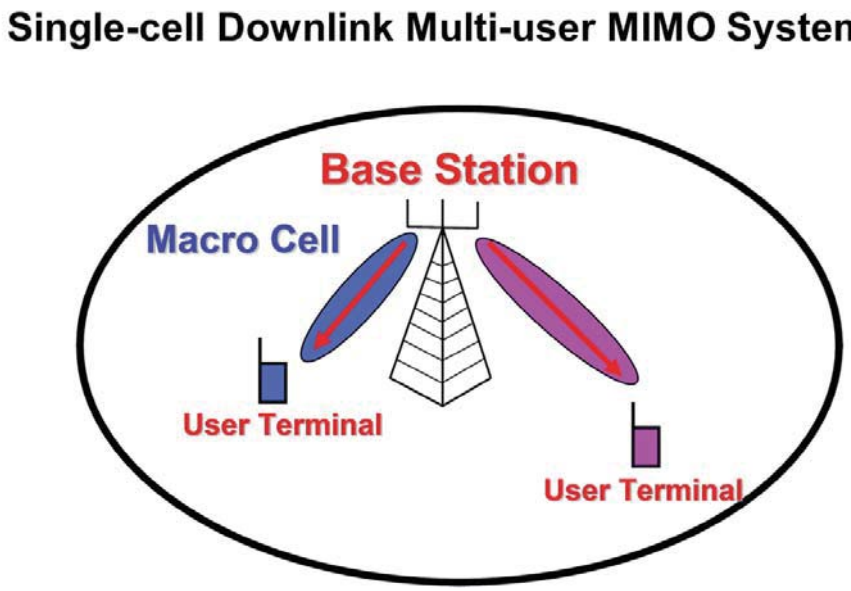

FIGURE 3.3: A Single-cell Downlink Massive MIMO System[4]

As we can see in Fig 1.1 and 3.3, this wireless powered communication system is consisted of single base station with number of M antennas which are serving number of K single-antenna wireless receivers with identical source. It is assumed to be in ideal channel state information(CSI) and Rayleigh fading massive MIMO channel is used. The channel vector between the BS and the k_{th} receiver are denoted as h_k and H is representing channel matrix. All the elements in H are identically distributed complex Gaussian parameters with zero mean and single variance and not dependent to each other. W is denoting the matrix of system beamforming and the linear precoding vector of k_{th} user is represented as w_k.

According to [86][87], the vector of the receiver is expressed by:

$$y = \sqrt{P_d} H_x + n = \sqrt{P_d} HWS + n \tag{3.9}$$

Where x is the vector of the transmitter, P_d is the overall power in downlink transmission power, n is the AGWN which stands for additive Gaussian white noise and S stands for the sensor signal matrix. The size of H is K $\times$ M and the size of W is

M × K. After the linear beamforming or precoding scheme the signal harvested by the k_{th} user can be expressed as:

$$y_k = \sqrt{P_d} h_k w_k s_k + \sqrt{P_d} \sum_{i=1}^{k} h_k w_i s_i + n \tag{3.10}$$

where $\sqrt{P_d} h_k w_k s_k$ is the ideal signal interfered by $\sqrt{P_d} \sum_{i=1}^{k} h_k w_i s_i$ and the noise is denoted as n.

As it's shown in [86], the SINR which is signal-to-interference-plus-noise ratio of the k_{th} user is given by[86]

$$SINR_K = \frac{P_d |h_k w_k|^2}{P_d \sum_{i=1}^{k} |h_k w_i|^2 + 1} \tag{3.11}$$

This is a function of the vector for transmitting beamforming.

In the letter, two transitional linear beamforming or precoding schemes are discussed and compared: the Zero-Forcing beamformer scheme(ZF) and another one is Maximum Ration Transmission scheme. According to Equation 3.11, these two scheme has their own expression for SINR hence we would use these two different SINR in the following section 3.2.1.

3.2.1 Zero Forcing Beamforming Scheme

According to [88], by using the zero forcing beamforming (ZF) scheme the interference between users can be canceled out at every user hence the energy harvest process can be optimized by using less energy source.

ZF precoding used by the base station is expressed as [86]

$$W = H^H (H H^H)^{-1} \tag{3.12}$$

For relatively large enough number of K and M, the related SINR of k_{th} user is expressed as [89]

$$SINR_K^{zf} = P_d (\frac{M - K}{K}) \tag{3.13}$$

3.2.2 Maximum Ratio Transmission Precoding Scheme

According to [88], by utilizing the maximum ratio transmission (MRT) scheme the signal gain at desired user can be maximized so the power consumption can be reduced thereby the energy receiving system is improved.

MRT precoding utilized by the base is given by [86]

$$W = H^H \tag{3.14}$$

For relatively large enough number of K and M, the related SINR of k_{th} user is expressed as [89]

$$SINR_K^{mrt} = \frac{P_d M}{K(P_d + 1)} \tag{3.15}$$

As shown in Equations 3.13 and 3.15, we can see that using same values of P_d, M and K in both cases, the SINR of two different schemes are still different. In order to achieve a proper performance comparison, SINR cannot be assigned same values in ZF and MRT schemes.

3.2.3 Achievable Data Rate

According to [86], achievable data rate (ADR) is one of the critical method used to quantify the wireless communication network performance. It's following the Shannon theorem which provides the largest data rate during the transmission procedure in the downlink network. In this part, we assign the same parameters of the overall downlink RF power and we assume that it's equally distributed to all receivers. In addition, all other parameters are set to under the same assumption. Therefore, by using this theorem the expression of the channel capacity over AWGN channel can by obtained as [89]

$$R = log_2(1 + SNR)(bits/s/Hz) \tag{3.16}$$

In Equation 3.16, SNR stands for signal-to-noise ratio. In wireless powered communication systems, channel state information (CSI) is an essential term. Basically,

energy are transmitted from the base station to each receivers selectively and concurrently with CSI[90]. Afterwards, channel feedback from all the sensors or receivers are sent back to the transmitter in uplink link so the base station can obtain the CSI. Thus, a ideal CSI in built up in the transmission network. As we can see in Equation 3.16, the receiving signal by every user is composed of additive white Gaussian nosie and the interfering signal between each user. Therefore, the ADR of each user in the wireless communication MIMO system with ideal CSI can be expressed as [89]

$$R_k = log_2(1 + SINR_k) \tag{3.17}$$

For all of these users, the achievable sum rate can be expressed as

$$R_{sum} = Klog_2(1 + SINR_k) \tag{3.18}$$

3.2.3.1 The Achievable Sum Rate with ZF Scheme

In the case of Zero Forcing scheme, achievable sum can be obtained as [86]

$$R_{sum}^{zf} = Klog_2(1 + SINR_k^{zf}) \tag{3.19}$$

By substituting 3.13 into 3.19, we can further get:

$$R_{sum}^{zf} = Klog_2[1 + P_d(\frac{M - K}{K})] \tag{3.20}$$

3.2.3.2 The Achievable Sum Rate with MRT Scheme

In the case of maximum ratio transmission, achievable sum can be obtained as [86]

$$R_{sum}^{mrt} = Klog_2(1 + SINR_k^{mrt}) \tag{3.21}$$

By substituting 3.15 into 3.21, we can further get:

$$R_{sum}^{mrt} = Klog_2[1 + \frac{P_d M}{K(P_d + 1)}] \tag{3.22}$$

It can be seen that in Equation 3.20 and 3.22 same assumption and parameter values are assigned. When the value of transmit antenna M $\gg$ K, ZF scheme can obtain better data rate comparing to MRT precoding scheme.

3.2.4 Downlink Transmitting Power

In this section, the achievable sum rate is assigned to be the same in ZF and MRT schemes in order to achieve the same condition. The downlink transmitting power is otherwise considered as a variable since it's a significant measurement scale of the power efficiency. A more energy efficient communication system consumes less power to achieve the same quality of service. According to [86], for the purpose of derivation, we represent

$$\alpha = \frac{M}{K} \tag{3.23}$$

And

$$\alpha - 1 = \frac{M - K}{K} \tag{3.24}$$

3.2.4.1 Downlink Transmitting Power with ZF

Substituting Equation 3.24 into 3.20 and given the ASR in both linear transmission schemes are identical, we can get

$$\begin{aligned} R_{sum} &= Klog_2[1 + P_d^{zf}(\alpha - 1)] \\ &\Rightarrow ln[1 + P_d^{zf}(\alpha - 1)] = ln2(\frac{R_{sum}}{K}) \end{aligned} \tag{3.25}$$

Exponential can be taken in the both sides of the equation:

$$P_d^{zf} = \frac{e^{\frac{ln2 R_{sum}}{k} - 1}}{\alpha - 1} \tag{3.26}$$

Substituting Equation 3.24 into 3.26 gives

$$P_d^{zf} = K[\frac{e^{\frac{ln2R_{sum}}{k}-1}}{M-K}] \tag{3.27}$$

This gives the overall downlink transmitting power with Zero Forcing scheme.

3.2.4.2 Downlink Transmitting Power with MRT

Using the same method as used for the last scheme, we substitute Equation 3.23 into 3.22 and yields:

$$R + sum = Klog_2(1 + \frac{p_d^{mrt}\alpha}{P_d^{mrt}+1}) \tag{3.28}$$

Exponential can be taken in the both sides of the equation:

$$P_d^{mrt} = \frac{e^{\frac{ln2R_{sum}}{K}-1}}{\alpha - [e^{\frac{ln2R_{sum}}{K}} - 1]} \tag{3.29}$$

Substituting Equation 3.23 into 3.29 yields:

$$P_d^{mrt} = \frac{e^{\frac{ln2R_{sum}}{K}-1}}{\frac{M}{K} - [e^{\frac{ln2R_{sum}}{K}} - 1]} \tag{3.30}$$

$$P_d^{mrt} = \frac{K[e^{\frac{ln2R_{sum}}{K}-1}]}{M - K[e^{\frac{ln2R_{sum}}{K}} - 1]} \tag{3.31}$$

Because of the overall downlink transmitting power is considered to be identically distributed to all the receivers and same as the achievable sum rate. There are three cases are learned from [86] for our computation, considering three different parameter values conditions in Equation 3.27 and 3.31.

1. First Case: Assuming the overall power is demanded to achieve **exactly one** bit per second per Hz for every user. That is:

$$\begin{aligned} R_{sum} = K, e^{\frac{ln2R_{sum}}{K}} = e^{ln2} = 2 \\ \Rightarrow M - K[e^{\frac{ln2R_{sum}}{K}} - 1] = M - K \end{aligned} \tag{3.32}$$

   According to this assumption and from the Equation 3.27, 3.31 and 3.32, we can give a conclusion that:

$$P_d^{zf} = P_d^{mrt}$$

   With same amount of power divided among every users, even with M $\gg$ K, the overall downlink transmitting power is same for both cases.

2. Second Case: Assuming the overall power is demanded to achieve **more than one** bit per second per Hz for every user. That is:

$$\begin{aligned} R_{sum} > K, \text{ which yields} \\ P_d^{mrt} > P_d^{zf} \end{aligned}$$

   According to this assumption, we can make a conclusion that for ASR uniformly distributed among every user, as the total number of the transmitting antennas raise to M $\gg$ K, ZF is requiring less energy than MRT to achieve the same amount of energy for every user. It implies that ZF has higher power efficiency while achieving higher data rate.

3. Third Case: Assuming the overall power is demanded to achieve **less than one** bit per second per Hz for every user. That is:

$$\begin{aligned} R_{sum} < K, \text{ which yields} \\ P_d^{mrt} < P_d^{zf} \end{aligned}$$

   According to this assumption, we can make a conclusion that for ASR uniformly distributed among every user, as the total number of the transmitting antennas raise to M $\gg$ K, MRT is requiring less energy than ZF to achieve the same amount of energy for every user. It implies that MRT has higher power efficiency while achieving lower data rate.

Chapter 4

Simulation Results

4.1 Energy Harvesting

4.1.1 Energy Harvesting Stage One

In the first stage, the process of transmitting energy from the base station to the receivers is simulated and analyzed. The simulated result in Fig. 4.1 shows the behavior of the charging procedure during the energy transmission process. As we can see in the figure, when we increase the input RF transmitting power from 0W to 70mW, the output RF power is actually saturated when the input power reach around 40mW. This illustrate that the our proposed non-linear energy harvesting model for practical energy harvesting circuit wireless energy harvesting is coinciding with the experimental result provided in [91] and [92]. Moreover. this result also implies that linear mode proposed by [93] [94] [95] [96] and [97] is not precise for modeling a non-linear energy harvesting circuit.

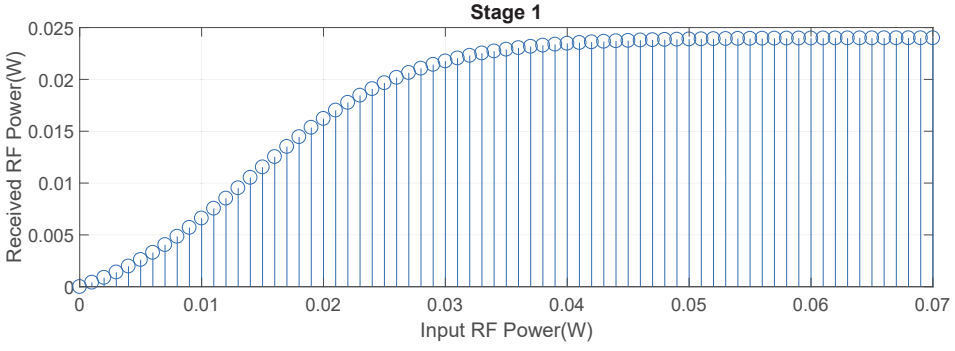

FIGURE 4.1: Behavior of stage one charging process

4.1.2 Energy Harvesting Stage Two

In the second stage, the energy harvested from the transmitter is utilized in the receivers and a functional block name P1110 is employed to simulate the energy harvesting process. As we can see in Fig. 3.1, the voltage across the load is V_{OUT}, which is equal to to the supply voltage in Fig. 3.2. Therefore, charging this P1110 functional block is equivalently charging the equivalent normal R-C circuit as shown in Fig. 3.2. The capacitor here can be regarded as a normal sensor which is fetching energy from the base station. As long as we can find out the relationship between the input RF power from the base station, the charging time and the output RF power delivered to the supercapacitor, we can be acquainted with the characteristic of the charging procedure and by utilizing these features we can control the behavior of the sensors. As a result, it could significantly simplify and optimize the design procedure of RF charging via wireless communication network hence power consumptions can be reduced to relatively low level.

In the simulation process, Equation 3.8 is utilized and firstly we set the range of time from 0 to 1s and choose a fixed value of P_{IN} and try to find out the relationship between charging time and the harvested RF power across the supercapacitor. Afterwards, we gradually increase the input RF power from the base station in order to find out the relationship of these three variables. As we can see in Fig. 4.2, as the charging time increases to around 0.9s, the harvest output RF power is saturated even with different input RF power P_{IN}. This comply with the same relationship comparing to the charging procedure in stage one. Moreover, Fig. 4.2 also illustrate a well-known rule that when input RF power P_{IN} is increased, the output power would be increased accordingly.

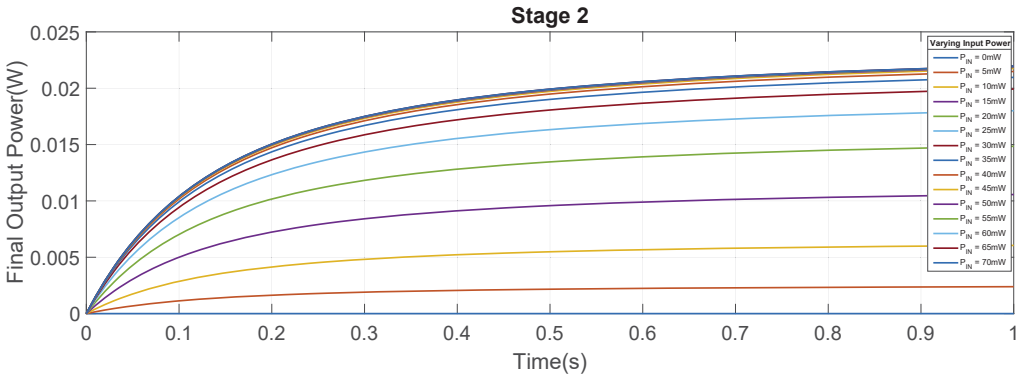

FIGURE 4.2: Behavior of stage two charging process with different values of input RF power

4.1.3 Three-dimensional Simulation Result

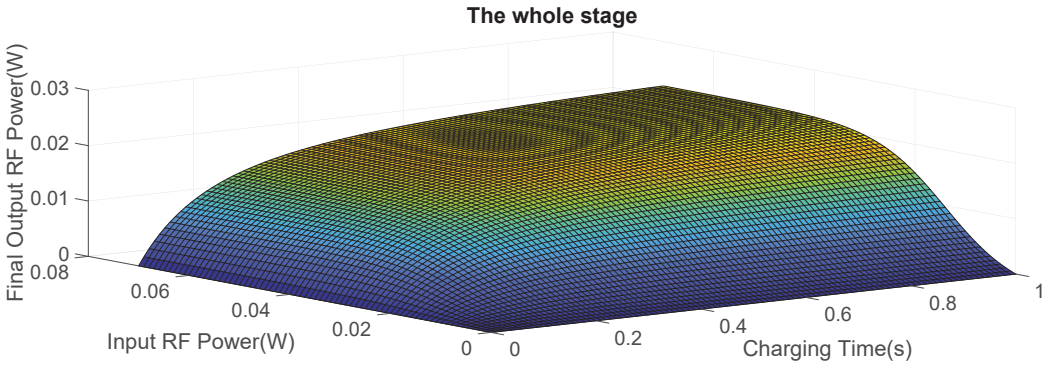

FIGURE 4.3: Proposed Three-dimensional Model

As we can see in Fig. 4.3, it's describing the relationship between the charging time, input BS RF power and output capacitor RF power. Upon utilizing the characteristics and behavior of this three dimension energy harvesting model, we can ultimately control the output RF power consumption by designing certain among of input RF power and/or certain charging time. In addition to this, if we are given a input RF power from the base station and the time period to charge certain device, we can easily work out the final output RF power the device is using.

4.2 Resource Allocation

4.2.1 Achievable Sum Rate with ZF and MRT

For the purpose of proving and validating the theoretical and experimental result discussion in chapter3, simulations is conducted using same conditions and assumptions. In Fig. 4.4, the overall downlink transmitting power available is 15dB and the number of receivers K is equal to 10.

The relationship between the number of transmitting antennas and the overall achievable sum rate is shown in Fig. 4.4. Firstly, it can be obviously seen that the achievable rum rate would increase as the number of base station increases in both ZF and MRT schemes. Moreover, from the comparison of these two sets of data it can be seen that ZF can obtain much greater sum rate than MRT. For the range of 20 to 200 transmitting antennas, the achievable sum rate of ZF is two times, almost three times greater than MRT. As a result, it can be concluded that

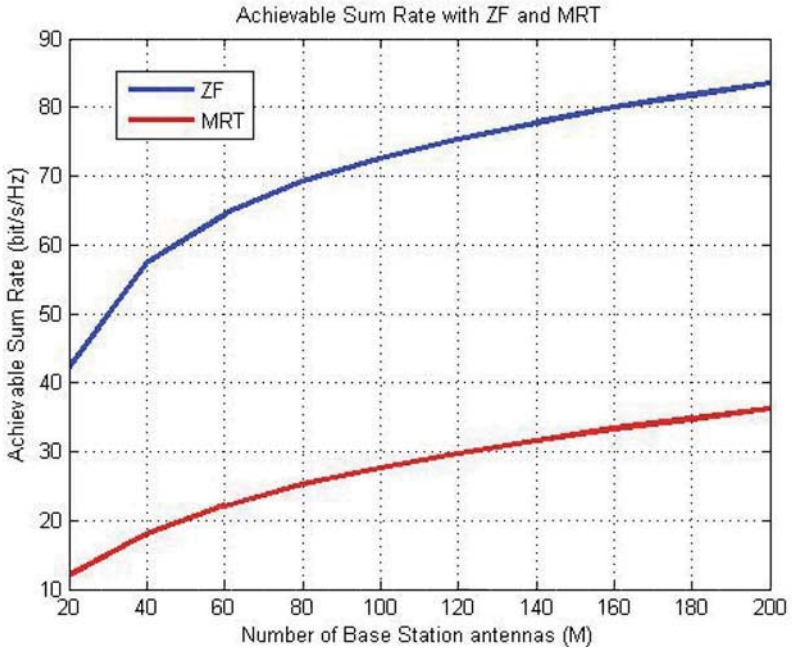

FIGURE 4.4: Behavior Comparison of Total Achievable Rate versus the Number of Base Station Antennas

ZF can achieve significantly much greater data transmission rate comparing to MRT scheme where the input base station transmitting power is shared uniformly among every user.

4.2.2 Overall Downlink Transmitting Power with ZF and MRT

Fig. 4.5 4.6 and 4.7 demonstrate the relationship between overall downlink transmitting power and the number of transmitting antennas. In all of these three cases the number of wireless receivers(users) K is 10, however the desired achieved sum rate is different in each case.

1. Case One

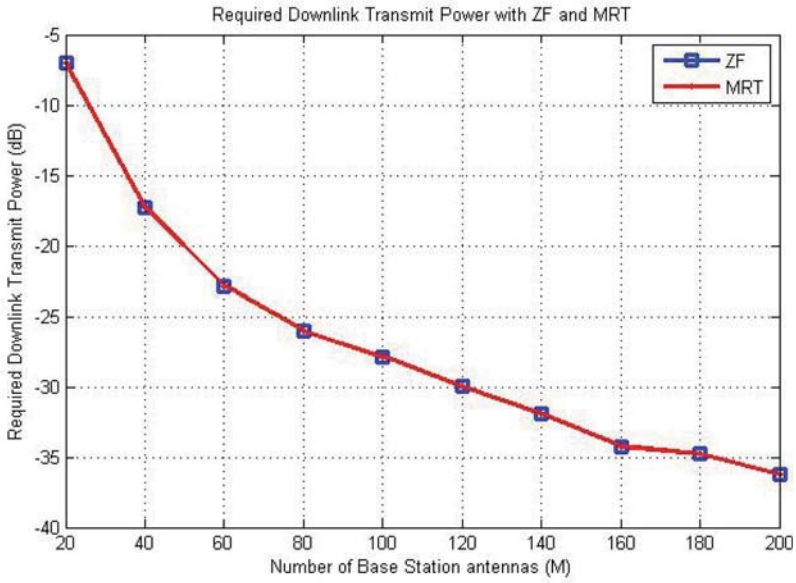

FIGURE 4.5: Behavior comparison of overall transmitting power acquired to achieve **exactly one** bit/s/Hz for every user

2. Case Two

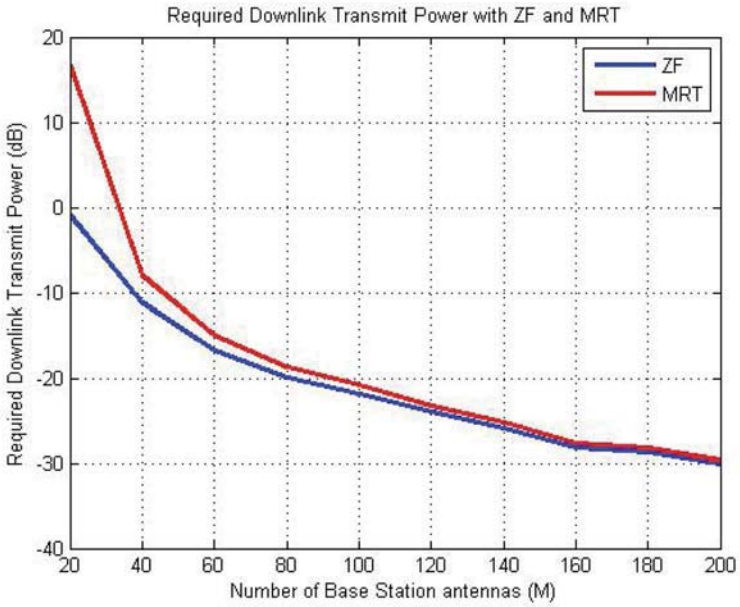

FIGURE 4.6: Behavior comparison of overall transmitting power acquired to achieve **more than one** bit/s/Hz for every user

3. Case Three

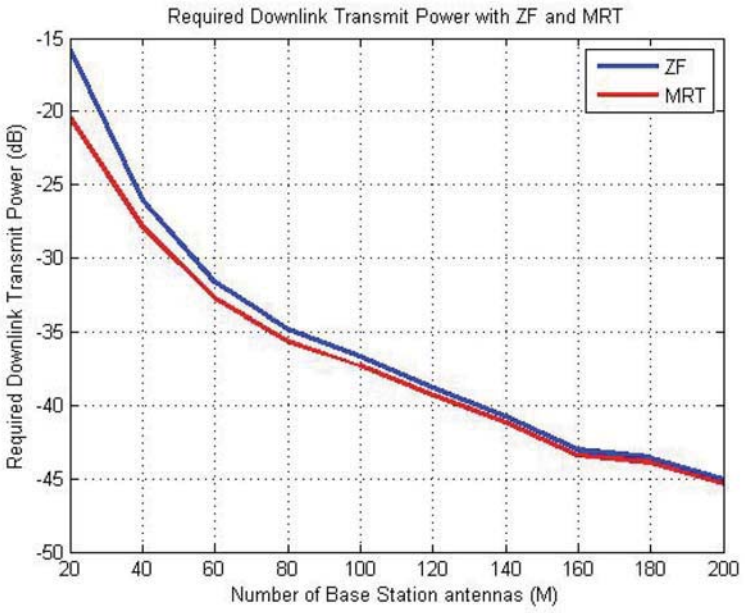

FIGURE 4.7: Behavior comparison of overall transmitting power acquired to achieve **less than one** bit/s/Hz for every user

As we can see from Fig 4.5 4.6 and 4.7, although in these cases the overall downlink transmitting power for two linear precoding schemes are not as diverse as the achievable sum rate, there is still some difference of their behavior in resource allocation process. In Fig 4.5, the downlink transmitting power is acquired to obtain **exactly one** bit/s/Hz for every receiver and the desired achieved sum rate is 10 bits per second per Hz. In Fig 4.6, the downlink transmitting power is acquired to obtain **more than one** bit/s/Hz for every receiver and the desired achieved sum rate is 15 bits per second per Hz. In Fig 4.7, the downlink transmitting power is acquired to obtain **less than one** bit/s/Hz for every receiver and the desired achieved sum rate is 5 bits per second per Hz.

In general, as the number of base station increase, the overall downlink transmitting power drop down for all of these three cases. Specifically, in Fig 4.5 the overall required power for two precoding schemes are same but in Fig 4.6 the ZF transmission scheme acquire less power to achieve the desired sum rate and the condition is opposite in Fig 4.7. Simulations results for three cases are coinciding with the theoretical result discussed in section 3.

4.2.3 Achieved Sum Rate Versus Downlink Transmitting Power

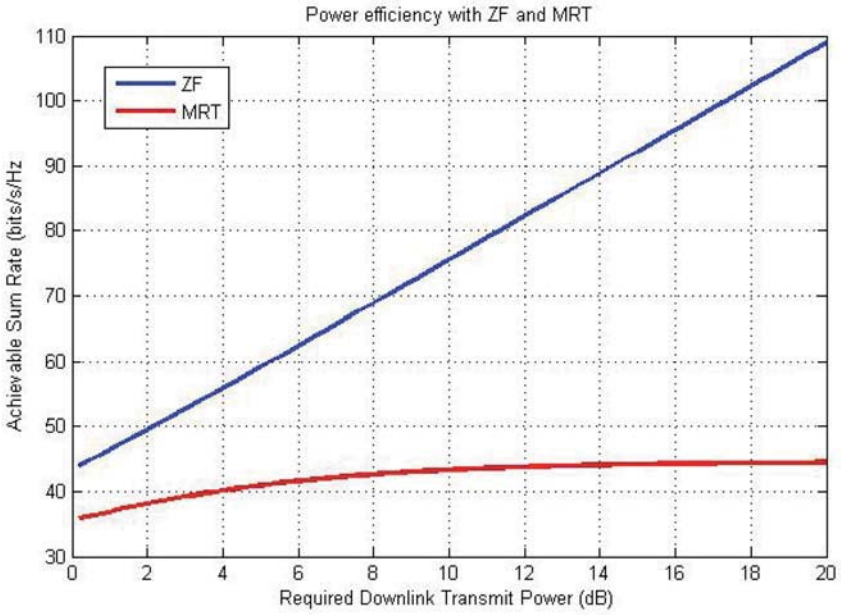

FIGURE 4.8: Power Efficiency Comparison of ZF and MRT

In the end, the relationship between the achieved sum rate (ASR) and the overall downlink transmitting power (DTP) is analyzed. The results illustrate that in the same level of overall downlink transmitting power (in the range of 0 to 20 decibel), much greater data transmission rate is achieved by ZF scheme comparing to MRT. The ASR is greater than the number of wireless receivers, which means that the resource allocation scheme is being run under the second case that we discussed above in section 4.2.2. Therefore, each user is utilizing the power more than 1 bits/s/Hz thereby we can conclude that Zero Forcing scheme has less power consumption and utilize the power more efficiently.

Chapter 5

Conclusion

In conclusion, one of the most potential solution to provide sustained network operation to ambient sensor nodes ins the devoted RF energy source. Its different from conventional constant supply voltage charging since its providing steady power from the supply source to the storage element. The characterization in charging procedure to demonstrate the behavior of RF energy transfer procedure has been analyzed and obtained thereby the relationship between charging time, input power and output power is derived.

Moreover, the behavior of two linear precoding schemes ZF and MRT are analyzed and compared in different perspectives. The main characteristics has been analyzed are the achievable sum rate and overall downlink transmit power which are obtained under the same condition and assumptions. In addition to this, simulation results further support and validate the previous study and show that ZF can obtain greater data rate comparing to MRT. Therefore, we can summarize that ZF is a better choice in the wireless powered communication MIMO system. In the future, we could further extend our analysis to both downlink and uplink area or the multi-cells MIMO system.

Bibliography

[1] E. Boshkovska, D. W. K. Ng, N. Zlatanov, and R. Schober, "Practical non-linear energy harvesting model and resource allocation for swipt systems," *IEEE Communications Letters*, vol. 19, no. 12, pp. 2082–2085, 2015.

[2] Y. Sun, D. W. K. Ng, Z. Ding, and R. Schober, "Optimal joint power and subcarrier allocation for full-duplex multicarrier non-orthogonal multiple access systems," *IEEE Transactions on Communications*, vol. 65, no. 3, pp. 1077–1091, March 2017.

[3] D. Mishra, S. De, and K. R. Chowdhury, "Charging time characterization for wireless rf energy transfer," *IEEE Transactions on Circuits and Systems II: Express Briefs*, vol. 62, no. 4, pp. 362–366, 2015.

[4] "Mobile communications networking." [Online]. Available: http://www.nec-labs.com/research-departments/mobile-communications/mobile-communications-projects/advanced-mimo-communication

[5] D. W. K. Ng, E. S. Lo, and R. Schober, "Energy-Efficient Resource Allocation in OFDMA Systems with Hybrid Energy Harvesting Base Station," *IEEE Trans. Wireless Commun.*, vol. 12, pp. 3412–3427, Jul. 2013.

[6] I. Ahmed, A. Ikhlef, D. W. K. Ng, and R. Schober, "Power Allocation for an Energy Harvesting Transmitter with Hybrid Energy Sources," *IEEE Trans. Wireless Commun.*, vol. 12, pp. 6255–6267, Dec. 2013.

[7] V. Raghunathan, A. Kansal, J. Hsu, J. Friedman, and M. Srivastava, "Design considerations for solar energy harvesting wireless embedded systems," in *Proceedings of the 4th international symposium on Information processing in sensor networks*. IEEE Press, 2005, p. 64.

[8] Y. K. Tan and S. K. Panda, "Optimized wind energy harvesting system using resistance emulator and active rectifier for wireless sensor nodes," *IEEE transactions on power electronics*, vol. 26, no. 1, pp. 38–50, 2011.

[9] S. P. Beeby, M. J. Tudor, and N. White, "Energy harvesting vibration sources for microsystems applications," *Measurement science and technology*, vol. 17, no. 12, p. R175, 2006.

[10] P. Grover and A. Sahai, "Shannon Meets Tesla: Wireless Information and Power Transfer," in *Proc. IEEE Intern. Sympos. on Inf. Theory*, Jun. 2010, pp. 2363 –2367.

[11] J. O. McSpadden, L. Fan, and K. Chang, "Design and experiments of a high-conversion-efficiency 5.8-ghz rectenna," *IEEE Transactions on Microwave Theory and Techniques*, vol. 46, no. 12, pp. 2053–2060, 1998.

[12] I. Krikidis, S. Timotheou, S. Nikolaou, G. Zheng, D. W. K. Ng, and R. Schober, "Simultaneous Wireless Information and Power Transfer in Modern Communication Systems," *IEEE Commun. Mag.*, vol. 52, no. 11, pp. 104–110, Nov. 2014.

[13] Z. Ding, C. Zhong, D. W. K. Ng, M. Peng, H. A. Suraweera, R. Schober, and H. V. Poor, "Application of Smart Antenna Technologies in Simultaneous Wireless Information and Power Transfer," *IEEE Commun. Mag.*, vol. 53, no. 4, pp. 86–93, Apr. 2015.

[14] X. Chen, Z. Zhang, H.-H. Chen, and H. Zhang, "Enhancing Wireless Information and Power Transfer by Exploiting Multi-Antenna Techniques," *IEEE Commun. Mag.*, no. 4, pp. 133–141, Apr. 2015.

[15] X. Chen, D. W. K. Ng, and H.-H. Chen, "Secrecy Wireless Information and Power Transfer: Challenges and Opportunities," *IEEE Commun. Mag.*, 2016.

[16] Q. Wu, M. Tao, D. Ng, W. Chen, and R. Schober, "Energy-Efficient Resource Allocation for Wireless Powered Communication Networks," *IEEE Trans. Wireless Commun.*, vol. 15, pp. 2312–2327, 2016.

[17] X. Chen, X. Wang, and X. Chen, "Energy-Efficient Optimization for Wireless Information and Power Transfer in Large-Scale MIMO Systems Employing Energy Beamforming," *IEEE Wireless Commun. Lett.*, vol. 2, pp. 1–4, Dec. 2013.

[18] D. W. K. Ng, E. S. Lo, and R. Schober, "Wireless Information and Power Transfer: Energy Efficiency Optimization in OFDMA Systems," *IEEE Trans. Wireless Commun.*, vol. 12, pp. 6352–6370, Dec. 2013.

[19] R. Zhang and C. K. Ho, "MIMO Broadcasting for Simultaneous Wireless Information and Power Transfer," *IEEE Trans. Wireless Commun.*, vol. 12, pp. 1989–2001, May 2013.

[20] S. Leng, D. W. K. Ng, N. Zlatanov, and R. Schober, "Multi-Objective Resource Allocation in Full-Duplex SWIPT Systems," in *Proc. IEEE Intern. Commun. Conf.*, 2016.

[21] D. W. K. Ng, E. S. Lo, and R. Schober, "Robust Beamforming for Secure Communication in Systems with Wireless Information and Power Transfer," *IEEE Trans. Wireless Commun.*, vol. 13, pp. 4599–4615, Aug. 2014.

[22] D. W. K. Ng and R. Schober, "Secure and Green SWIPT in Distributed Antenna Networks with Limited Backhaul Capacity," *IEEE Trans. Wireless Commun.*, vol. 14, no. 9, pp. 5082–5097, 2015.

[23] M. Khandaker and K.-K. Wong, "Robust Secrecy Beamforming With Energy-Harvesting Eavesdroppers," *IEEE Wireless Commun. Lett.*, vol. 4, pp. 10–13, Feb. 2015.

[24] D. W. K. Ng, E. S. Lo, and R. Schober, "Multi-Objective Resource Allocation for Secure Communication in Cognitive Radio Networks with Wireless Information and Power Transfer," to appear in *IEEE Trans. Veh. Technol.*, May 2015.

[25] Q. Wu, W. Chen, and J. Li, "Wireless Powered Communications With Initial Energy: QoS Guaranteed Energy-Efficient Resource Allocation," *IEEE Wireless Commun. Lett.*, vol. 19, Dec. 2015.

[26] S. Kisseleff, I. F. Akyildiz, and W. Gerstacker, "Beamforming for Magnetic Induction Based Wireless Power Transfer Systems with Multiple Receivers," in *Proc. IEEE Global Telecommun. Conf.*, Dec. 2015, pp. 1–7.

[27] S. Kisseleff, X. Chen, I. F. Akyildiz, and W. Gerstacker, "Wireless Power Transfer for Access Limited Wireless Underground Sensor Networks," in *Proc. IEEE Intern. Commun. Conf.*, May 2016.

[28] S. Kisseleff, X. Chen, I. F. Akyildiz, and W. H. Gerstacker, "Efficient Charging of Access Limited Wireless Underground Sensor Networks," *IEEE Trans. Commun.*, vol. 64, no. 5, pp. 2130–2142, May 2016.

[29] P. Niu, P. Chapman, R. Riemer, and X. Zhang, "Evaluation of motions and actuation methods for biomechanical energy harvesting," in *Power Electronics Specialists Conference, 2004. PESC 04. 2004 IEEE 35th Annual*, vol. 3. IEEE, 2004, pp. 2100–2106.

[30] Z. A. Eu, W. K. Seah, and H.-P. Tan, "A study of mac schemes for wireless sensor networks powered by ambient energy harvesting," in *Proceedings of the 4th Annual International Conference on Wireless Internet*. ICST (Institute for Computer Sciences, Social-Informatics and Telecommunications Engineering), 2008, p. 78.

[31] H. Visser, "Indoor wireless rf energy transfer for powering wireless sensors," *Radioengineering*, 2012.

[32] S. De and R. Singhal, "Toward uninterrupted operation of wireless sensor networks," *Computer*, vol. 9, no. 45, pp. 24–30, 2012.

[33] R. C. Shah, S. Roy, S. Jain, and W. Brunette, "Data mules: Modeling and analysis of a three-tier architecture for sparse sensor networks," *Ad Hoc Networks*, vol. 1, no. 2, pp. 215–233, 2003.

[34] T. Kim and W. Qiao, "A hybrid battery model capable of capturing dynamic circuit characteristics and nonlinear capacity effects," *IEEE Transactions on Energy Conversion*, vol. 26, no. 4, pp. 1172–1180, 2011.

[35] J. Fitzpatrick, "Simulation of a wireless mimo system," 2004. [Online]. Available: https://www.scribd.com/document/57622633/Ofdm-Thesis-Simulation-of-a-Wireless-MIMO-System-2004

[36] E. G. Larsson, O. Edfors, F. Tufvesson, and T. L. Marzetta, "Massive mimo for next generation wireless systems," *IEEE Communications Magazine*, vol. 52, no. 2, pp. 186–195, 2014.

[37] R. W. Heath Jr, "What is the role of mimo in future cellular networks: Massive? coordinated? mmwave?" in *Presentation delivered at Int. Conf. on Communi.(ICC)*, 2013.

[38] C. Han, T. Harrold, S. Armour, I. Krikidis, S. Videv, P. M. Grant, H. Haas, J. S. Thompson, I. Ku, C.-X. Wang *et al.*, "Green radio: radio techniques to enable energy-efficient wireless networks," *IEEE communications magazine*, vol. 49, no. 6, 2011.

[39] Z. Zheng, X. Zhang, L. X. Cai, R. Zhang, and X. Shen, "Sustainable communication and networking in two-tier green cellular networks," *IEEE Wireless Communications*, vol. 21, no. 4, pp. 47–53, 2014.

[40] D. W. K. Ng, E. S. Lo, and R. Schober, "Energy-Efficient Resource Allocation in Multi-Cell OFDMA Systems with Limited Backhaul Capacity," *IEEE Trans. Wireless Commun.*, vol. 11, pp. 3618–3631, Oct. 2012.

[41] D. W. K. Ng, E. Lo, and R. Schober, "Energy-Efficient Resource Allocation in OFDMA Systems with Large Numbers of Base Station Antennas," *IEEE Trans. Wireless Commun.*, vol. 11, pp. 3292 –3304, Sep. 2012.

[42] Q. Wu, W. Chen, M. Tao, J. Li, H. Tang, and J. Wu, "Resource Allocation for Joint Transmitter and Receiver Energy Efficiency Maximization in Downlink OFDMA Systems," *IEEE Trans. Commun.*, vol. 63, pp. 416–430, Feb. 2015.

[43] Q. Wu, M. Tao, and W. Chen, "Joint Tx/Rx Energy-Efficient Scheduling in Multi-Radio Wireless Networks: A Divide-and-Conquer Approach," *IEEE Trans. Wireless Commun.*, vol. 15, pp. 2727–2740, Apr. 2016.

[44] Q. Wu, W. Chen, and J. Li, "Wireless powered communications with initial energy: QoS guaranteed energy-efficient resource allocation," vol. 19, no. 12, pp. 2278 – 2281, Dec. 2015.

[45] Q. Wu, W. Chen, J. Li, and J. Wu, "Low complexity energy-efficient design for OFDMA systems with an elaborate power model," in *Proc. IEEE GLOBECOM*, 2014, Accepted.

[46] Q. Wu, W. Chen, D. W. K. Ng, J. Li, and R. Schober, "User-centric energy efficiency maximization for wireless powered communications," vol. 15, no. 19, pp. 6898 – 6912, Jul. 2016.

[47] Q. Wu, W. Chen, M. Tao, J. Li, H. Tang, and J. Wu, "Resource allocation for joint transmitter and receiver energy efficiency maximization in downlink OFDMA systems," vol. 63, no. 2, pp. 416–430, Feb. 2015.

[48] Q. Wu, G. Y. Li, W. Chen, and D. W. K. Ng, "Energy-efficient small cell with spectrum-power trading," vol. 34, no. 12, pp. 3394–3408, Dec. 2016.

[49] Q. Wu, G. Y. Li, W. Chen, D. W. K. Ng, and R. Schober, "An overview of sustainable green 5G networks," 2017, [Online] Available: https://arxiv.org/abs/1609.09773.

[50] Q. Wu, M. Tao, and W. Chen, "Joint Tx/Rx energy-efficient scheduling in multi-radio wireless networks: A divide-and-conquer approach," to appear, 2015.

[51] ——, "Joint Tx/Rx energy-efficient scheduling in multi-radio wireless networks: A divide-and-conquer approach," in *Proc. IEEE ICC*, 2015, pp. 2476 – 2481.

[52] Q. Wu, M. Tao, W. Chen, and J. Wu, "Optimal energy-efficient transmission for fading channels with an energy harvesting transmitter," in *Proc. IEEE GLOBECOM*, 2014, Accepted.

[53] Q. Wu, M. Tao, D. W. K. Ng, W. Chen, and R. Schober, "Energy-efficient resource allocation for wireless powered communication networks," vol. 15, no. 3, pp. 2312–2327, Mar. 2016.

[54] ——, "Energy-efficient transmission for wireless powered multiuser communication networks," in *Proc. IEEE ICC*, 2015, pp. 154–159.

[55] Q. Wu, Y. Zeng, and R. Zhang, "Joint trajectory and communication design for UAV-enabled multiple access," submitted to IEEE GLOBECOM 2017, [Online] Available: arXiv preprint arXiv:1704.01765.

[56] Y. Wu, J. Wang, L. Qian, and R. Schober, "Optimal power control for energy efficient D2D communication and its distributed implementation," vol. 19, no. 5, pp. 815–818, May 2015.

[57] H. Bogucka and A. Conti, "Degrees of freedom for energy savings in practical adaptive wireless systems," *IEEE Communications Magazine*, vol. 49, no. 6, 2011.

[58] R. V. Prasad, S. Devasenapathy, V. S. Rao, and J. Vazifehdan, "Reincarnation in the ambiance: Devices and networks with energy harvesting," *IEEE Communications Surveys & Tutorials*, vol. 16, no. 1, pp. 195–213, 2014.

[59] I. Krikidis, S. Timotheou, S. Nikolaou, G. Zheng, D. W. K. Ng, and R. Schober, "Simultaneous wireless information and power transfer in modern communication systems," *IEEE Communications Magazine*, vol. 52, no. 11, pp. 104–110, 2014.

[60] D. Gunduz, K. Stamatiou, N. Michelusi, and M. Zorzi, "Designing intelligent energy harvesting communication systems," *IEEE Communications Magazine*, vol. 52, no. 1, pp. 210–216, 2014.

[61] S. Chen, P. Sinha, N. B. Shroff, and C. Joo, "Finite-horizon energy allocation and routing scheme in rechargeable sensor networks," in *INFOCOM, 2011 Proceedings IEEE*. IEEE, 2011, pp. 2273–2281.

[62] S. Sudevalayam and P. Kulkarni, "Energy harvesting sensor nodes: Survey and implications," *IEEE Communications Surveys & Tutorials*, vol. 13, no. 3, pp. 443–461, 2011.

[63] M. Gorlatova, P. Kinget, I. Kymissis, D. Rubenstein, X. Wang, and G. Zussman, "Energy harvesting active networked tags (enhants) for ubiquitous object networking," *IEEE Wireless Communications*, vol. 17, no. 6, 2010.

[64] ——, "Energy harvesting active networked tags (enhants) for ubiquitous object networking," *IEEE Wireless Communications*, vol. 17, no. 6, 2010.

[65] O. Ozel and S. Ulukus, "Achieving awgn capacity under stochastic energy harvesting," *IEEE Transactions on Information Theory*, vol. 58, no. 10, pp. 6471–6483, 2012.

[66] A. A. Nasir, X. Zhou, S. Durrani, and R. A. Kennedy, "Relaying protocols for wireless energy harvesting and information processing," *IEEE Transactions on Wireless Communications*, vol. 12, no. 7, pp. 3622–3636, 2013.

[67] H. S. Dhillon, Y. Li, P. Nuggehalli, Z. Pi, and J. G. Andrews, "Fundamentals of heterogeneous cellular networks with energy harvesting," *IEEE Transactions on Wireless Communications*, vol. 13, no. 5, pp. 2782–2797, 2014.

[68] M. Zheng, P. Pawelczak, S. Stanczak, and H. Yu, "Planning of cellular networks enhanced by energy harvesting," *IEEE Communications Letters*, vol. 17, no. 6, pp. 1092–1095, 2013.

[69] L. Liu, R. Zhang, and K.-C. Chua, "Wireless information transfer with opportunistic energy harvesting," *IEEE Transactions on Wireless Communications*, vol. 12, no. 1, pp. 288–300, 2013.

[70] X. Zhou, R. Zhang, and C. K. Ho, "Wireless Information and Power Transfer: Architecture Design and Rate-Energy Tradeoff," in *Proc. IEEE Global Telecommun. Conf.*, Dec. 2012.

[71] D. W. K. Ng, E. S. Lo, and R. Schober, "Energy-Efficient Resource Allocation in Multiuser OFDM Systems with Wireless Information and Power Transfer," in *Proc. IEEE Wireless Commun. and Netw. Conf.*, 2013.

[72] S. Leng, D. W. K. Ng, and R. Schober, "Power Efficient and Secure Multiuser Communication Systems with Wireless Information and Power Transfer," in *Proc. IEEE Intern. Commun. Conf.*, Jun. 2014.

[73] D. W. K. Ng, L. Xiang, and R. Schober, "Multi-Objective Beamforming for Secure Communication in Systems with Wireless Information and Power Transfer," in *Proc. IEEE Personal, Indoor and Mobile Radio Commun. Sympos.*, Sep. 2013.

[74] D. W. K. Ng, R. Schober, and H. Alnuweiri, "Secure Layered Transmission in Multicast Systems With Wireless Information and Power Transfer," in *Proc. IEEE Intern. Commun. Conf.*, Jun. 2014, pp. 5389–5395.

[75] D. W. K. Ng and R. Schober, "Resource Allocation for Coordinated Multipoint Networks With Wireless Information and Power Transfer," in *Proc. IEEE Global Telecommun. Conf.*, Dec. 2014, pp. 4281–4287.

[76] M. Chynonova, R. Morsi, D. W. K. Ng, and R. Schober, "Optimal Multiuser Scheduling Schemes for Simultaneous Wireless Information and Power Transfer," in *23rd European Signal Process. Conf. (EUSIPCO)*, Aug. 2015.

[77] Q. Wu, M. Tao, D. W. K. Ng, W. Chen, and R. Schober, "Energy-Efficient Transmission for Wireless Powered Multiuser Communication Networks," in *Proc. IEEE Intern. Commun. Conf.*, Jun. 2015.

[78] T. A. Le, Q. T. Vien, H. X. Nguyen, D. W. K. Ng, and R. Schober, "Robust Chance-Constrained Optimization for Power-Efficient and Secure SWIPT Systems," *IEEE Transactions on Green Communications and Networking*, vol. PP, no. 99, pp. 1–1, 2017.

[79] E. Boshkovska, D. W. K. Ng, N. Zlatanov, A. Koelpin, and R. Schober, "Robust Resource Allocation for MIMO Wireless Powered Communication Networks Based on a Non-Linear EH Model," *IEEE Trans. Commun.*, vol. 65, no. 5, pp. 1984–1999, May 2017.

[80] D. Ng and R. Schober, "Max-Min Fair Wireless Energy Transfer for Secure Multiuser Communication Systems," in *IEEE Inf. Theory Workshop (ITW)*, Nov 2014, pp. 326–330.

[81] L. Fu, P. Cheng, Y. Gu, J. Chen, and T. He, "Minimizing charging delay in wireless rechargeable sensor networks," in *INFOCOM, 2013 Proceedings IEEE*. IEEE, 2013, pp. 2922–2930.

[82] Z. Li, Y. Peng, W. Zhang, and D. Qiao, "J-roc: a joint routing and charging scheme to prolong sensor network lifetime," in *2011 19th IEEE International Conference on Network Protocols*. IEEE, 2011, pp. 373–382.

[83] M. A. Guerrero, E. Romero, F. Barrero, M. I. Milans, and E. Gonzlez, "Supercapacitors: alternative energy storage systems," *Przegld Elektrotechniczny*, vol. 85, no. 10, pp. 188–195, 2009.

[84] P. Kulsangcharoen, C. Klumpner, M. Rashed, and G. Asher, "A new duty cycle based efficiency estimation method for a supercapacitor stack under constant power operation," in *Power Electronics, Machines and Drives (PEMD 2010), 5th IET International Conference on*. IET, 2010, pp. 1–6.

[85] "Powercast p1110 powerharvester receiver datasheet." [Online]. Available: http://www.powercastco.com/PDF/P1110-datasheet.pdf

[86] T. Parfait, Y. Kuang, and K. Jerry, "Performance analysis and comparison of zf and mrt based downlink massive mimo systems," in *Ubiquitous and Future Networks (ICUFN), 2014 Sixth International Conf on*. IEEE, 2014, pp. 383–388.

[87] M. A. Mohammad, A. A. Osman, and N. A. Elhag, "Performance comparison of mrt and zf for single cell downlink massive mimo system," in *Computing, Control, Networking, Electronics and Embedded Systems Engineering (ICCNEEE), 2015 International Conference on*. IEEE, 2015, pp. 52–56.

[88] E. Pakdeejit, "Linear precoding performance of massive mu-mimo downlink system," 2013.

[89] S. Choi, "Massive mimo ppt," Jun 2012. [Online]. Available: https://wenku.baidu.com/view/9f2ae6f1fab069dc5022014a.html

[90] T. L. Marzetta and B. M. Hochwald, "Fast transfer of channel state information in wireless systems," *IEEE Transactions on Signal Processing*, vol. 54, no. 4, pp. 1268–1278, 2006.

[91] T. Le, K. Mayaram, and T. Fiez, "Efficient far-field radio frequency energy harvesting for passively powered sensor networks," *IEEE Journal of Solid-State Circuits*, vol. 43, no. 5, pp. 1287–1302, 2008.

[92] J. Guo and X. Zhu, "An improved analytical model for rf-dc conversion efficiency in microwave rectifiers," in *Microwave Symposium Digest (MTT), 2012 IEEE MTT-S International*. IEEE, 2012, pp. 1–3.

[93] I. Krikidis, S. Timotheou, S. Nikolaou, G. Zheng, D. W. K. Ng, and R. Schober, "Simultaneous wireless information and power transfer in modern communication systems," *IEEE Communications Magazine*, vol. 52, no. 11, pp. 104–110, 2014.

[94] X. Chen, Z. Zhang, H.-H. Chen, and H. Zhang, "Enhancing wireless information and power transfer by exploiting multi-antenna techniques," *IEEE Communications Magazine*, vol. 53, no. 4, pp. 133–141, 2015.

[95] R. Zhang and C. K. Ho, "Mimo broadcasting for simultaneous wireless information and power transfer," *IEEE Transactions on Wireless Communications*, vol. 12, no. 5, pp. 1989–2001, 2013.

[96] D. W. K. Ng, E. S. Lo, and R. Schober, "Wireless information and power transfer: Energy efficiency optimization in ofdma systems," *IEEE Transactions on Wireless Communications*, vol. 12, no. 12, pp. 6352–6370, 2013.

[97] X. Chen, X. Wang, and X. Chen, "Energy-efficient optimization for wireless information and power transfer in large-scale mimo systems employing energy beamforming," *IEEE Wireless Communications Letters*, vol. 2, no. 6, pp. 667–670, 2013.

Appendix A

MATLAB Code

Three-Dimension Model

```
clear all;
close all;
clc;
%% Defining Variables
R = 3;
C = 50e-3;
t = 0:0.01:1;
i = 1;
a = 150;
b = 0.014;
M = 0.024;
p_inbefore = 0:1e-3:70e-3;
%% Passing the sensor
for p_inb4 = p_inbefore(1:length(p_inbefore))
legendInfo{i} = ['P_{IN} = ' num2str(p_inb4*1e3) 'mW'];
PP = M ./(1 + exp(-a .*(p_inb4 - b)));
Ohm = 1/(1+exp(a*b));
p_inafter(i) = (PP - M.*Ohm)./(1-Ohm);
%stem(p, p_inafter(i));
i = i+1;
%hold on
end
figure
stem(p_inbefore, p_inafter);
%hold off
xlabel('Input RF Power(W)')
ylabel('Received RF Power(W)')
title('Stage 1')
i = 1;
%% Pasing the capacitor
figure
for P_IN = p_inafter(1:length(p_inafter))
W0 = lambertw(0,exp(1.+(2.*t)./(R.*C)));
Z = 0.5.*(1.+W0);
```

```
Q = 2.*C.*sqrt(R.*P_IN).*(1-1./Z)./sqrt(1-(1-1./Z).^2);
V = (2.*sqrt(R.*P_IN).*(1.-1./Z))./sqrt(1.-(1.-1./Z).^2);
I = ((-Q./C)+sqrt((Q./C).^2.+4.*R.*P_IN))./(2.*R);
P_OUT(i,:) = I.*V;
plot(t,P_OUT(i,:));
%stem(p_in,P_IN);
hold on
i = i + 1;
end
hold off
xlabel('Time(s)')
ylabel('Final Output RF Power(W)')
title('Stage 2')
legend(legendInfo);

%% 3D view
figure
surf(t,p_inbefore,P_OUT);
xlabel('Time(s)')
ylabel('Input RF Power(W)')
zlabel('Final Output RF Power(W)')
title('The whole stage')
%cftool(t,p_inbefore,P_OUT)
```

Stage One Curve Fitting Result VS Original Curve

```
clear all;
close all;
clc;
R = 3;
C = 50e-3;
t = 0.5;
a = 150;
b = 0.014;
M = 0.024;
% p_inbefore = 10e-3:
% p_inbefore = 200e-3;
% PP = M ./(1 + exp(-a .*(p_inbefore - b)));
% Ohm = 1/(1+exp(a*b));
i = 1;
p_inbefore= 0:1e-3:70e-3;
% p_inafter = (PP - M.*Ohm)./(1-Ohm);
PP = M ./(1 + exp(-a .*(p_inbefore - b)));
Ohm = 1/(1+exp(a*b));
p_inafter = (PP - M.*Ohm)./(1-Ohm);
P_IN = p_inafter;
W0 = lambertw(0,exp(1.+(2.*t)./(R.*C)));
Z = 0.5.*(1.+W0);
Q = 2.*C.*sqrt(R.*P_IN).*(1-1./Z)./sqrt(1-(1-1./Z).^2);
V = (2.*sqrt(R.*P_IN).*(1.-1./Z))./sqrt(1.-(1.-1./Z).^2);
I = ((-Q./C)+sqrt((Q./C).^2.+4.*R.*P_IN))./(2.*R);
P_OUT = I.*V;
%legendInfo{i} = ['P_{IN} = ' num2str(P_IN)];
```

```
figure
plot(p_inbefore,p_inafter);
hold on
plot(p_inbefore,P_OUT,'--');

%stem(p_in,P_IN);
xlabel('Input Power(W)')
ylabel('Output Power(W)')
title('Output Power versus Input Power')
%legend(legendInfo);
```

Stage Two Curve Fitting Result VS Original Curve

```
%% ploting the data
clear all;
close all;
clc;
R = 3;
C = 50e-3;
t = 0:0.01:1;
% a = 150;
% b = 0.014;
% M = 0.024;
i = 1;
p_inbefore = 1;
P_IN = p_inbefore;
W0 = lambertw(0,exp(1.+(2.*t)./(R.*C)));
Z = 0.5.*(1.+W0);
Q = 2.*C.*sqrt(R.*P_IN).*(1-1./Z)./sqrt(1-(1-1./Z).^2);
V = (2.*sqrt(R.*P_IN).*(1.-1./Z))./sqrt(1.-(1.-1./Z).^2);
I = ((-Q./C)+sqrt((Q./C).^2.+4.*R.*P_IN))./(2.*R);
P_OUT = I.*V;
%legendInfo{i} = ['P_{IN} = ' num2str(P_IN)];
%plot(t,P_OUT);
% x = t;
% y = P_OUT;
%% Using the coefficients from the curve fitting result (using curve
%% fitting tool)
a1 =  10.46;
b1 = 0.1239;
M1 = 0.8755;
PP = M1 ./(1 + exp(-a1 .*(t - b1)));
Ohm = 1/(1+exp(a1*b1));
P_OUT2 = (PP - M1.*Ohm)./(1-Ohm);
figure
plot(t,P_OUT,'ko',t,P_OUT2,'-b');
legend('Data','Fitted curve');
%hold on
% y2 = 3.3778e15./(1.2538e17.*(exp(2.1 - 150.*x) + 1)) - 0.0029;
% plot(x,y,'ko',x,y2,'-b');
xlabel('Time(s)')
ylabel('Output Power(W)')
title('Output Power versus Time When P_{IN} = 1W')
```

```
% legend(legendInfo);
```

Stage2 Simulation

```
clear all;close all;clc;
R = 3;
C = 50e-3;
t = 0:0.01:1;
i = 1;
a = 150;
b = 0.014;
M = 0.024;
p_inbefore = 0:1:70;
% figure
% for p_inb4 = p_inbefore(1:length(p_inbefore))
% PP = M ./(1 + exp(-a .*(p_inb4 - b)));
% Ohm = 1/(1+exp(a*b));
% p_inafter(i) = (PP - M.*Ohm)./(1-Ohm);
% %stem(p, p_inafter(i));
% i = i+1;
% hold on
% end
% %plot(p_inbefore, p_after);
% hold off
% % xlabel('Input Power Before(W)')
% % ylabel('Input Power After(W)')
% % title('Before and After')
i = 1;
figure
for P_IN = p_inbefore(1:length(p_inbefore))
W0 = lambertw(0,exp(1.+(2.*t)./(R.*C)));
Z = 0.5.*(1.+W0);
Q = 2.*C.*sqrt(R.*P_IN).*(1-1./Z)./sqrt(1-(1-1./Z).^2);
V = (2.*sqrt(R.*P_IN).*(1.-1./Z))./sqrt(1.-(1.-1./Z).^2);
I = ((-Q./C)+sqrt((Q./C).^2.+4.*R.*P_IN))./(2.*R);
P_OUT(i,:) = I.*V;
plot(t,P_OUT(i,:));
%stem(p_in,P_IN);
hold on
%legendInfo{i} = ['P_IN = ' num2str(P_IN)];
i = i + 1;
end
hold off
xlabel('Time(s)')
ylabel('Output Power(W)')
title('Output Power versus Time with different Input Power')
%legend(legendInfo);
figure
surf(t,p_inbefore,P_OUT);
xlabel('Time(s)')
ylabel('Input Power(W)')
zlabel('Output Power(W)')
title('Pout VS Pin VS Time')
```